JTTEE5 19:476–483
DOI: 10.1007/s11666-009-9439-6
1059-9630/$19.00 © ASM International

Estimation of Molten Content of the Spray Stream from Analysis of Experimental Particle Diagnostics

Vasudevan Srinivasan and Sanjay Sampath

(Submitted June 29, 2009; in revised form October 9, 2009)

Particle melting is one of the key issues in air plasma spray processing of high temperature ceramics such as Yttria Stabilized Zirconia (YSZ). The significance of assessing, monitoring, and controlling the molten content in spray stream on achieving an efficient process and reproducible coating characteristics and properties is known. This study aims to estimate the molten content of the spray stream (as an ensemble) from experimental measurement of in-flight (individual) particle characteristics. In a previous study by Streibl et al. the presence of melting signature in the particle temperature distribution was observed, which has been confirmed by simulation and through independent experimental observation by Mauer et al. Based on this observation, the particle temperature distribution could be delineated into the different achievable particle states in-flight (unmolten, partially molten, and completely molten) to a first approximation. This in-turn would enable estimation of the molten content in the spray stream. Thus obtained percentage molten content (referred in this study as Spray Stream Melting Index—SSMI) has been observed to correlate well with the experimentally measured deposition efficiency for a wide range of process conditions and feedstock characteristics. The implications of estimating SSMI for other materials and processes are also discussed.

Keywords deposition efficiency, in-flight particle diagnostics, molten content, particle melting, plasma spray processing, temperature distribution

1. Introduction

Dependence of coating microstructure and properties on particle state is well documented and so is the dependence of particle state on direct (torch parameters and particle injection) and indirect (nozzle wear and associated voltage drop) process conditions (Ref 1). In plasma spray processing of high melting point low thermal conductivity materials melting of particles is a concern. Particle melting is a concern not only with respect to obtaining good melting and deposition efficiency but also in achieving the desired coating microstructure and properties consistently.

Monitoring and controlling the process in real-time based on particle state is widely accepted as a reasonable strategy to achieve consistent particle state and coating characteristics (other parameters such as substrate conditions remaining constant) (Ref 2-4). In-flight sensors have made possible the measurement of temperature (T), velocity (V), and assessment of size (D) of individual particles as well as ensemble temperature, velocity, size, shape, and trajectory of the spray stream. But due to the dynamic nature of the spray stream it becomes necessary to understand and comprehensively describe the spray stream in order to rely entirely on in-flight parameters for monitoring and controlling the process. Studies have suggested the importance of temperature, velocity, and molten state/fraction of the spray stream as important characteristics describing the spray stream (Ref 5, 6). But it has not been possible to measure or calculate/assess the molten content of spray stream based on in-flight data until now. This is because the extent of melting of a particle or molten content is not a directly measurable parameter (at least using commercially available sensors) and typically flame-related parameters have to be calculated numerically (Ref 7) to assess molten content.

Insufficiency of particle temperature to describe the particle's thermal state at the individual particle level is well established. Attempts have been made to extract more information from measured particle data and parameters such as Melting Index have been proposed (Ref 7). Yet at the spray stream level studies have suggested that average temperature and velocity control the

This article is an invited paper selected from presentations at the 2009 International Thermal Spray Conference and has been expanded from the original presentation. It is simultaneously published in *Expanding Thermal Spray Performance to New Markets and Applications: Proceedings of the 2009 International Thermal Spray Conference*, Las Vegas, Nevada, USA, May 4-7, 2009, Basil R. Marple, Margaret M. Hyland, Yuk-Chiu Lau, Chang-Jiu Li, Rogerio S. Lima, and Ghislain Montavon, Ed., ASM International, Materials Park, OH, 2009.

Vasudevan Srinivasan and **Sanjay Sampath**, Department of Materials Science and Engineering, Center for Thermal Spray Research, Stony Brook University, 130 Heavy Engineering Building, Stony Brook, NY 11794-2275. Contact e-mail: vsriniva.ctsr@gmail.com.

microstructure and properties of coatings to a first approximation (Ref 6, 8-10).

Careful consideration of the particle temperature distributions has revealed their multi-modal nature (Ref 11, 12), which raises the fundamental question whether average (temperature) is sufficient to describe the distribution. Further analysis of the distribution by fitting for the underlying sub-distributions has shown the presence of one sub-distribution at the same temperature, which has been verified to be the melting point of the material (Ref 11, 13).

These observations in temperature distributions present an interesting opportunity to understand the melting status of spray stream as a whole. Toward comprehensive description of the spray stream we explore the possibility of calculating molten fraction based on analysis of temperature distributions from individual particle measurements in this study.

2. Experimental Details

APS 7MB torch (Sulzer Metco, Westbury, NY) with an 8 mm 'G' nozzle was used with non-swirl gas distribution. A mixture of nitrogen (N_2) and hydrogen (H_2) gas was used for plasma generation throughout this study due to the higher enthalpy of the gas combination and the associated benefits of melting hard to melt materials such as YSZ. Particles were injected externally orthogonal to the spray axis top down into the plasma jet. Particle injection was optimized (constant trajectory) for all process conditions used throughout this study hence eliminating particle injection as a potential variable [More information available in reference (Ref 14)]. Angular morphology (fused and crushed) 8% YSZ (Saint-Gobain, Worcester, MA), Mn-Zn Ferrite (custom made), and Molybdenum (Global Tungsten Products, Towanda, PA) were chosen for the study. Process parameters used in this study are shown in Table 1.

Detailed in-flight diagnostics were performed using a suite of in-flight process sensors although the focus of this article is the analysis of data from measurements of individual particle T & V using DPV 2000 (Tecnar Ltd, St Bruno, Canada) (serial # DPV 0016; 18 mm lens; P4590170 mask; $\lambda 1 = 787 \pm 25$ nm and $\lambda 2 = 995 \pm 25$ nm). More information about DPV including equipment details, measurement principles, and error analysis can be found in references (Ref 11, 13, 15) and in DPV equipment manual. Data were collected from large number of particles (~10,000) at the flow center (particle flux) of the spray stream at the spray distance of 130 mm and their distribution analyzed. Distributions of particle temperature collected at the flow center of the spray stream and across the entire spray stream (spray stream cross section scan at the spray distance) are comparable once a large number of particles have been collected.

Deposits were made on grit blasted 3 mm thick Al 6061 T6 substrates of dimensions 225 by 25 mm^2 mounted on in situ coating curvature sensor ICP [for more information refer (Ref 10, 16-18)] at 130 mm standoff distance. Substrates were preheated to about 200 °C in all cases and the substrate temperature during deposition was between 240 °C and 280 °C (measured at the back of the substrate using contact thermocouple). The deposition procedure and all related parameters were maintained the same for all the experiments.

3. Results and Discussion

3.1 Analysis of Particle Temperature Distributions

Particle temperature distributions of YSZ have been observed to be tri-modal under most process conditions (considered in this study) and not a normal distribution as commonly assumed. This becomes clear when the underlying sub-distributions are fitted as Gaussian distributions G1 through G3 (to achieve maximum chi square) as shown in Fig. 1 (Table 1 exp E1). Peak P1 has been identified to occur at the same temperature (~2500 °C) for a wide variety of process conditions as shown in Fig. 2 (Table 1 exp E3) and validated to be the melting point of the material. The difference between observed melting temperature and equilibrium melting temperature (~200 °C) has been attributed to calibration of the sensor and the principle of measurement (Ref 11, 13). The location of peaks P2 and P3 vary depending on the process condition.

On a simpler note, if there are two process conditions with same average T but different V, the condition at lower velocity would be better melted due to longer dwell time in the plume. One such case is shown in Fig. 3 (Table 1 exp E2). It can be seen that the lower velocity condition has larger area under the Gaussian curves (G2 and G3) having peaks to the right of peak P1. This again shows that area under Gaussian curves with peaks to the right of peak P1 corresponds to the molten content in the spray stream and that the peak P1 itself corresponds to the melting point.

3.2 Spray Stream Melting Index: Molten Content of Spray Stream

Identifying the three possible states a particle can exhibit in-flight forms the basis for extracting molten content of spray stream.

(i) Completely molten: Particles have crossed the melting barrier (peak P1) and contribute to the sub-distributions on the higher temperature side

(ii) Unmolten: Particles have not crossed the peak (P1) and contribute to Gaussian sub-distributions on the low temperature side

(iii) Partially molten: Particles that contribute to the melting Gaussian curve (which houses peak P1) are partially molten, typically to varying extents

Spray Stream Melting Index (SSMI) is calculated as the ratio of sum of area under the completely molten peaks

Table 1 Process parameters used in this study

Experiment no.	Experiment description	Section in the article	Associated figure(s)	Powder	N_2 flow, slpm	H_2 flow, slpm	I, a	Power, kW
E1	Multimodal temperature distribution	Analysis of particle temperature distributions	Fig. 1	Saint-Gobain HW 1532(31-96 μm) *D*50 = 64	47.6	5.6	550	41
E2	Comparison of temperature distribution at same T but different V		Fig. 3		57.2 31.9	4.5 1.7	500 466	39 32
E3	Exploring process space - widely varying process condition	Spray Stream Melting Index to Estimate Deposition Efficiency	Fig. 2 Fig. 4		31.9-63.1	1.7-12.0	466-634	30-50
E4	Different particle size distribution		Fig. 5 Fig. 6	Saint-Gobain HW 1532 (31-96 μm) *D*50 = 64 HW 1622 (10-45 μm) *D*50 = 32 HW 1623 (45-75 μm) *D*50 = 61	47.6	5.6	550	41
E5	Process control based on average particle T & V	Spray Stream Melting Index to monitor/control the process	Fig. 7 Fig. 8 Fig. 9	Sulzer Metco 204 NS(HOSP) (27-95 μm) *D*50 = 60	41-53	1.7-12.0	434-706	36-48
E6	Molybdenum	Applicability of SSMI to other materials and processes	Fig. 10	SD 151 (55-77 μm) *D*50 = 63	31.9-63.1	1.7-12.0	466-634	30-50
E7	Ferrite (Mn-Zn Ferrite)	NA		Custom made/Proprietary				

Fig. 1 Typical particle temperature distribution for YSZ with the sub-distributions identified. G1, G2, and G3 refer to the Gaussian sub-distribution curves and P1, P2, and P3 refer to the respective peak locations. Refer Table 1 exp E1 for process parameters

and a factor of the area of the partially molten peak to the total area under the whole distribution.

$$\text{SSMI} = \left[(1 * A_{\text{m}}) + (0.5 * A_{\text{p}})\right] * 100/A \qquad \text{(Eq 1)}$$

where A_{m} is the area under the molten sub-distribution(s), A_{p} is the area under the partially molten sub-distribution, and A is the total area under the overall distribution. Fifty percent of particles under the partially molten distribution are assumed to be molten. The assumption is statistical in nature in that the mean (which on a relative scale is 50%) along with standard deviation ably represents a normal distribution while particles at different temperatures in the melting sub-distribution G1 would be molten to different extent.

3.3 Spray Stream Melting Index to Estimate Deposition Efficiency

Spray Stream Melting Index has been calculated for particle temperature distributions from two different sets of experiments (Table 1 exp E3 and exp E4) and related to deposition efficiency to understand the correlation. Relative deposition efficiency (RDE) has been calculated by normalizing the coating weight within each category of experiments compared in this study. Since the substrate and other conditions have not been changed this deposition efficiency represents the intrinsic process deposition efficiency which is a result of the particle state.

SSMI has been calculated for six widely varying process conditions exploring the safe operational process space in terms of the primary plasma-forming parameters namely primary gas flow, secondary gas flow, and arc current (for the given set of hardware). If one considers a simple L3 design of experiment cube with each of these three parameters along the independent mutually perpendicular

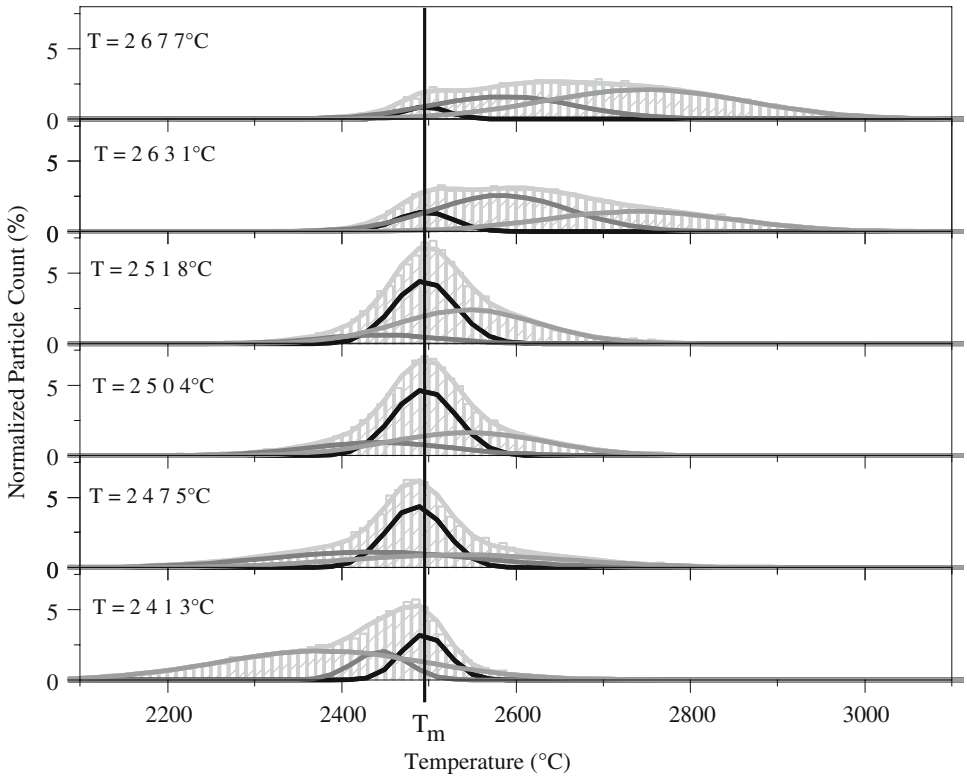

Fig. 2 Particle temperature distribution from process condition representing extremes of the safe operating space for YSZ. Shift in distribution from left to right can be observed with increasing average temperature, while the melting peak appears at the same temperature (T_m). Refer Table 1 exp E3 for process parameters

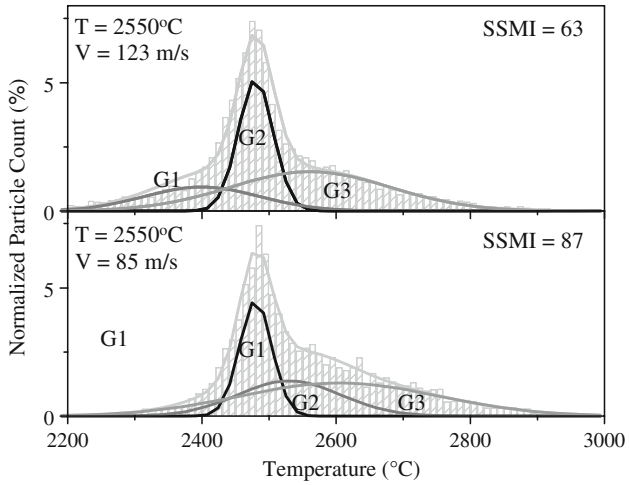

Fig. 3 Particle temperature distribution of YSZ at two different process conditions with same mean particle T but different mean V. Shift in sub-distributions can be observed, which forms the basis for Spray Stream Melting Index. In the distribution on top, particles in sub-distribution G1 are considered unmolten, particles in sub-distribution G2 are partially molten, and particles in sub-distribution G3 are fully molten. In the distribution at the bottom, particles in sub-distribution G1 are partially molten and particles in sub-distributions G2 and G3 are fully molten. Refer Table 1 exp E2 for process parameters

axis with the eight corners representing the safe operational limits, the resulting T-V space has been shown to be hexagonal in shape (Ref 10). Thus the six extreme conditions from T-V space have been used in this case to understand the correlation between particle state and deposition efficiency (Table 1 exp E3). One can observe the shift in temperature distribution (Fig. 2) as well as the wide range of SSMI and relative deposition efficiency (RDE) (Fig. 4) resulting from exploring the process space. Calculated SSMI appears to fit the observed RDE well implying the effectiveness of SSMI to estimate the deposition efficiency.

In another set of experiments (Table 1 exp E4), three angular morphology powders with different particle sizes were processed at the same torch parameters. The particle temperature distributions (Fig. 5) can be observed to be significantly different due to difference in extent of melting. SSMI fits the observed RDE extremely well ($R^2 \sim 1$) (Fig. 6). This again shows the effectiveness of SSMI to capture the molten state of the spray stream as a whole.

3.4 Spray Stream Melting Index to Monitor/Control the Process

In another series of experiments, very similar average particle T and V (±10 °C and ±2 m/s, respectively) were achieved by varying torch parameters widely for HOSP YSZ 204 NS material (see Table 1 exp E5 for the range of

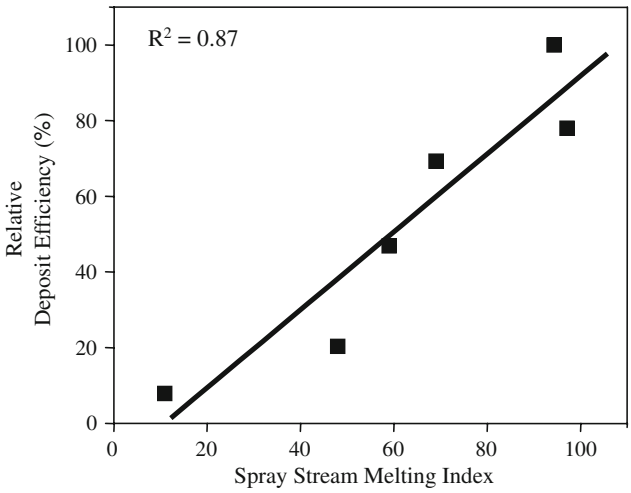

Fig. 4 Relation between calculated SSMI and observed relative deposition efficiency for a wide range of torch parameters for YSZ. Good fit indicates effectiveness of SSMI to capture the molten status of the spray stream in the considered case. Refer Table 1 exp E3 for process parameters

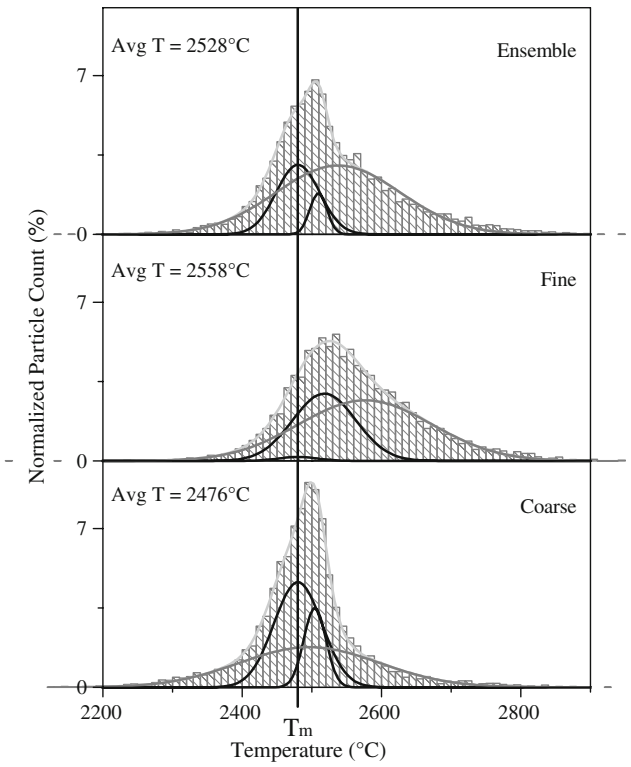

Fig. 5 Particle temperature distribution resulting from three different powder size distributions of YSZ material. The initial particle size distribution is as follows; Fine = 10-45 μm, Coarse = 45-75 μm, and Ensemble = 31-96 μm. Refer Table 1 exp E4 for process parameters

process conditions used to achieve the same average *T* and *V*). Despite achieving similar average particle *T* and *V*, significantly different particle temperature distribution,

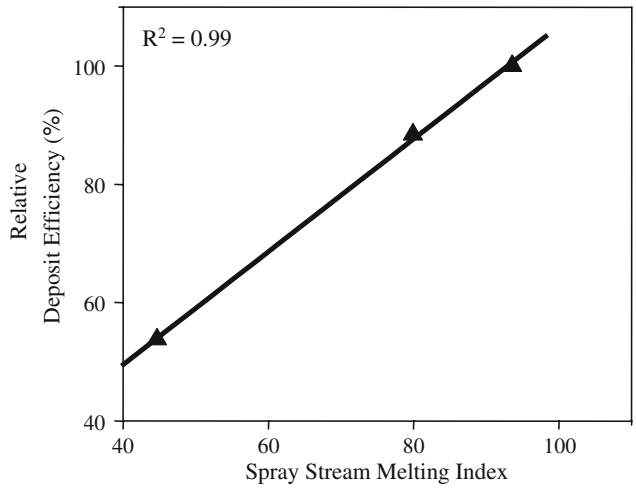

Fig. 6 Relation between calculated SSMI and observed RDE for three different powder size distributions of YSZ processed at the same process conditions. Very good fit can be observed (left to right on the SSMI scale are data from coarse, ensemble, and fine particle size distributions, respectively). Refer Table 1 exp E4 for process parameters

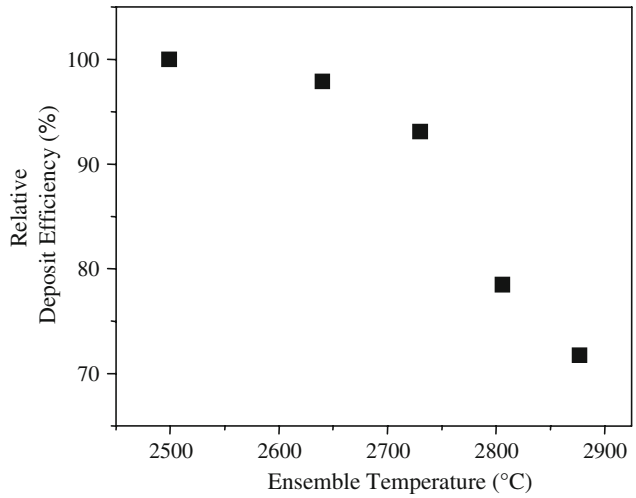

Fig. 7 Relation between deposition efficiency and ensemble temperature for YSZ when average particle *T* and *V* are similar. Reverse trend is observed (typically RDE would be expected to increase with increasing ensemble temperature). This brings up interesting issues of the ability of ensemble particle temperature to capture the characteristics of spray stream as well as the role of interference from particle vaporization on the ensemble measurements. Refer Table 1 exp E5 for process parameters

ensemble particle temperature and coating properties were observed. Measured *ensemble temperatures* could not explain the observed deposition efficiency (Fig. 7).

The subtle differences in particle temperature distribution quantified via SSMI shows good correlation to the observed deposition efficiency (Fig. 8). This shows the importance of considering the molten status of the spray stream to better describe the in-flight state of the process as well as the ability of SSMI to capture the molten status

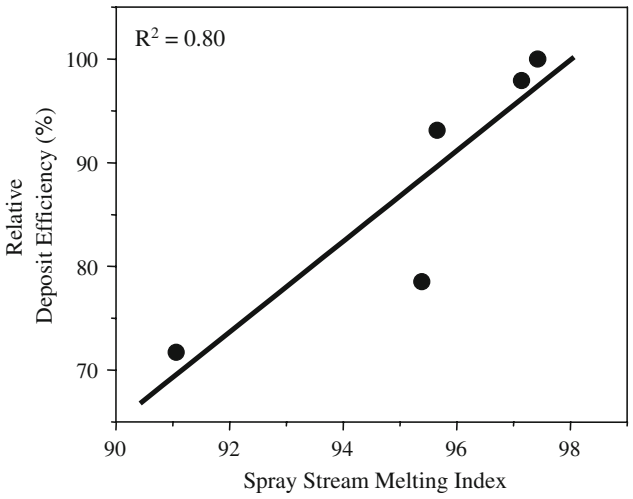

Fig. 8 Relation between calculated SSMI and observed RDE for YSZ when average particle *T* and *V* are similar. Good fit can be observed indicating that SSMI is a better parameter for capturing the in-flight state of the process. Refer Table 1 exp E5 for process parameters

of the spray stream. Further information on these experiments and additional inferences can be found in reference (Ref 11).

3.5 Scope and Limitations of Spray Stream Melting Index

In most cases involving plasma spray processing of TBCs SSMI can be used to estimate deposit efficiency as well as identify changes in process conditions for real-time process monitoring/control. It is applicable to any thermal spray process and material system that exhibits multi-modal distribution around melting point of the material (as determined from particle temperature distributions).

However, certain inherent limitations exist which need to be considered for appropriate interpretation of SSMI and for successful implementation in process state estimation/monitoring.

- When all the particles are either completely molten or unmolten, only shift in process can be identified using SSMI. Though the case of completely unmolten particles is very unlikely since it results in a highly uneconomical process, fully molten scenario is possible in a variety of cases. Materials with high thermal conductivity, low melting point, and/or fine particles all usually result in very high percentage of molten particles. SSMI can still be used to detect significant change in processing condition and to limited extent estimate deposit efficiency as well.
- The ability of particle temperature distribution to completely represent the spray stream is a concern when swirl gas flow is used, which results in time-dependent spatial variability of particle characteristics and at times result in more than one flow center compromising the accuracy of determining the flow center position.
- Limitations in particle sensing could lead to insufficiency of temperature distribution to completely describe the spray stream (e.g., particles < 5 μm, 'cold' particles and particles that vaporize significantly/with vapor cloud around them at the point of measurement are not measured).
- Contribution from unmolten particles to the coating buildup and deposition efficiency is not considered though one can observe unmolten particles in the coating microstructure to a small extent.
- In predicting deposition efficiency, the influence of substrate conditions (chemistry, roughness, temperature etc.…) is not accounted for. It is limited to assessing the influence of spray stream and in monitoring change in in-flight state of the process. The fit between RDE and SSMI could perhaps be improved by maintaining all other conditions identical.
- Sufficient number of particles (about 10,000) need to be acquired in order to be able to expose the sub-distributions which is necessary to calculate SSMI.

3.6 Applicability of SSMI to Other Materials and Processes

The observation of melting point in the temperature distribution is the key to identifying the three different states of particles in the spray stream. YSZ material system has the ideal blend of thermo-physical properties (low thermal conductivity, high melting point, and high emissivity) which makes observing the melting peak easy. Thus far, we have been able to calculate SSMI for YSZ processed under different conditions namely, different plasma gas combinations, plasma torch systems, feedstock size distributions, and different feedstock morphologies.

Under the right conditions, similar phenomenon can be observed in other material systems as well. Titania is one such material where despite the lower melting point and higher thermal conductivity (in comparison to YSZ), multi-modal distribution was observed when coarser particles were used. In such cases, SSMI can be used to estimate material relevant functional characteristics which are dependent on particle melting. We consider two different material systems here as an example.

Mn-Zn ferrite is a low melting material system, where one would not expect to observe the melting peak. But due to use of coarser feedstock in the size range of 20-200 μm (special sample feedstock), the signature melting peak could be observed by fitting the temperature distributions (Fig. 9). One of the key concerns in plasma spray processing of Ferrites is zinc loss due to vaporization, which influences the magnetic characteristics of the deposit in addition to deposition efficiency. The concept of SSMI can be used to estimate (to a first approximation) the amount of zinc loss and relative deposition efficiency after establishing appropriate correlations between the distribution and zinc loss despite the complexities of vaporization. Careful consideration is required for complete understanding of the particle temperature distribution where significant amount of vaporization happens.

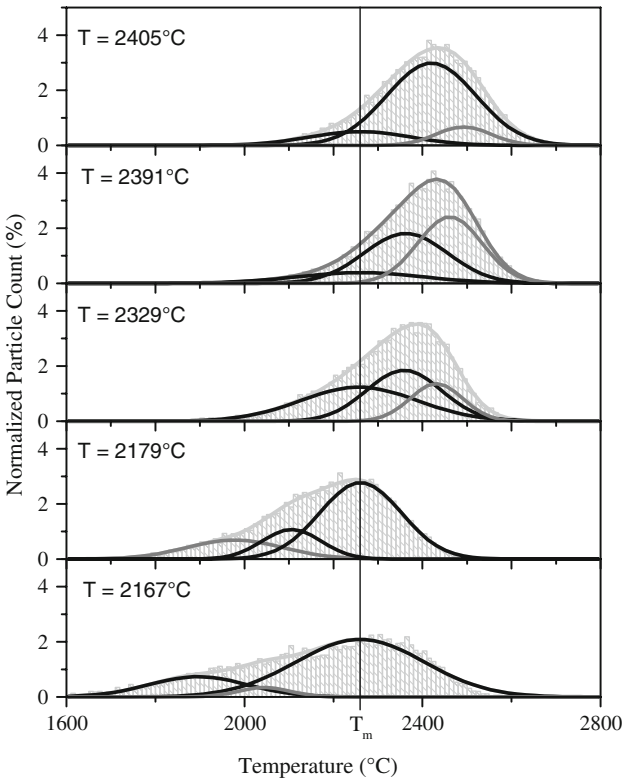

Fig. 9 Particle temperature distributions for Ferrite system. Melting peak can be observed to be stationary while the whole distribution shifts with processing condition. Refer Table 1 exp E5 for process parameters

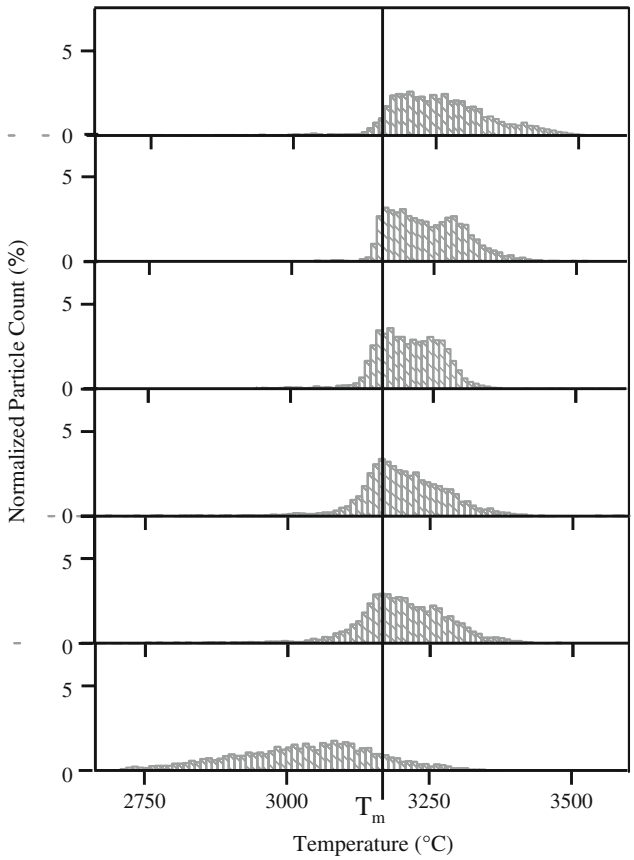

Fig. 10 Selected particle temperature distribution for Mo processed under different process conditions. Shift in distribution could be observed. Thus, SSMI can be calculated. Refer Table 1 exp E6 for process parameters

Guidance from process modeling is required and work is in progress toward understanding and establishing these correlations.

In another material system—Molybdenum—particle temperature distributions have been observed to shift in a similar fashion for the coarse powder (Fig. 10). Molybdenum is a higher melting point material (comparable to YSZ) with higher thermal conductivity (more than an order of magnitude higher than YSZ). Yet similar phenomenon can be observed in Molybdenum and hence, SSMI can be calculated. The two key issues in processing of this material system are melting and oxidation. Study is underway to understand the ability of SSMI to estimate deposition efficiency as well as the amount of oxidation.

4. Summary and Conclusion

In earlier studies done at the Center for Thermal Spray Research, in-flight particle temperature distributions have been observed to be multimodal. When fitted for underlying sub-distributions a signature of melting point has been observed. This presents an interesting opportunity to understand the melting status of particle and spray stream as a whole.

In this study, these multimodal temperature distributions were analyzed in an effort to quantify the distributions toward extracting the molten content of the spray stream which could be used toward comprehensive description of the spray stream.

The ratio of sum of area under the completely molten peaks and a factor of the area of the partially molten peak to the total area under the whole distribution represents the molten content in the spray stream. This approach provides a reliable quantitative representation of the molten content in the spray stream as a whole and hence the coined term Spray Stream Melting Index (SSMI).

SSMI calculated has been successfully calculated for a wide range of process conditions for YSZ (including feedstock size distributions). Moreover, SSMI has been shown to correlate well with the measured deposition efficiency (based on relative weight of coatings). This is an important finding given the significance of particle melting in splat formation and coating buildup.

It is clear that SSMI can be calculated and used for monitoring/controlling the in-flight state of the process for material systems that exhibit multimodal particle temperature distribution. It should be noted that SSMI by itself does not control the microstructure but plays a

critical role in understanding the microstructure and properties of coatings by enhancing the description of spray stream along with other in-flight particle thermal and momentum characteristics. Detailed microstructural characterization and property measurements have been done on the various YSZ coatings and effort is underway to establish comprehensive correlation between spray stream characteristics (thermal component, momentum component, and SSMI) and microstructure and properties. Studies are underway to understand the applicability of SSMI to other material systems toward estimating the influence of molten content of the spray stream on functional properties.

Acknowledgments

This work was supported by NSF MRSEC under award DMR 0080021, NSF GOALI FRG under award CMMI 0605704 and by the Industrial Consortium for Thermal Spray Technology at the Center for Thermal Spray Research.

References

1. P. Fauchais, Understanding Plasma Spraying, *J. Appl. Phys. D*, 2004, **37**(9), p R86-R108
2. M. Vardelle and P. Fauchais, Plasma Spray Processes: Diagnostics and Control?, *Pure Appl. Chem.*, 1999, **71**(10), p 1909-1918
3. C. Moreau, P. Gougeon, M. Lamontagne, V. Lacasse, G. Vaudreuil, and P. Cielo, On-Line Control of the Plasma Spraying Process by Monitoring the Temperature, Velocity and Trajectory of In-Flight Particles, *Thermal spray Industrial Applications: Proceedings of 7th National Thermal Spray Conference*, C.C. Berndt and S. Sampath, Ed., 1994 (Boston, MA, USA), ASM International, 1994, p 431-437
4. C. Moreau and L. Leblanc, Optimization and Process Control for High Performance Thermal Spray Coatings, *Durable Surf.*, 2001, **197**, p 27-57
5. J.R. Fincke, W.D. Swank, R.L. Bewley, D.C. Haggard, M. Gevelber, and D. Wroblewski, Diagnostics and Control in the Thermal Spray Process, *Surf. Coat. Technol.*, 2001, **146**, p 537-543
6. C. Moreau, Towards a Better Control of Thermal Spray, *Thermal Spray: Meeting the Challenges of the 21st Century*, C. Coddet, Ed., 1998 (Nice, France), ASM International, 1998, p 1677
7. H. Zhang, H.B. Xiong, L.L. Zheng, A. Vaidya, L. Li, and S. Sampath, Melting Behavior of In-flight Particles and Its Effects on Splat Morphology in Plasma Spraying, *International Mechanical Engineering Congress & Exposition*, Ed., 2002 (New Orleans, LA, United States), ASME International, 2002, p 309-316
8. M. Friis, C. Persson, and J. Wigren, Influence of Particle In-Flight Characteristics on the Microstructure of Atmospheric Plasma Sprayed Yttria Stabilized ZrO_2, *Surf. Coat. Technol.*, 2001, **141**(2-3), p 115-127
9. M. Prystay, P. Gougeon, and C. Moreau, Structure of Plasma-Sprayed Zirconia Coatings Tailored by Controlling the Temperature and Velocity of the Sprayed Particles, *J. Therm. Spray Technol.*, 2001, **10**(1), p 67-75
10. A. Vaidya, V. Srinivasan, T. Streibl, M. Friis, W. Chi, and S. Sampath, Process Maps for Plasma Spraying of Yttria-Stabilized Zirconia: An Integrated Approach to Design, Optimization and Reliability, *Mater. Sci. Eng. A*, 2008, **497**(1-2), p 239-253
11. T. Streibl, A. Vaidya, M. Friis, V. Srinivasan, and S. Sampath, A Critical Assessment of Particle Temperature Distributions during Plasma Spraying: Experimental Results for YSZ, *Plasma Chem. Plasma Process.*, 2006, **26**(1), p 73-102
12. S. Guessasma, G. Montavon, and C. Coddet, Velocity and Temperature Distributions of Alumina-Titania In-Flight Particles in the Atmospheric Plasma Spray Process, *Surf. Coat. Technol.*, 2005, **192**(1), p 70-76
13. G. Mauer, R. Vaßen, and D. Stöver, Detection of Melting Temperatures and Sources of Errors Using Two-Color Pyrometry During In-flight Measurements of Atmospheric Plasma-Sprayed Particles, *Int. J. Thermophys.*, 2008, **29**(2), p 764-786
14. V. Srinivasan, M. Friis, A. Vaidya, T. Streibl, and S. Sampath, Particle Injection in Direct Current Air Plasma Spray: Salient Observations and Optimization Strategies, *Plasma Chem. Plasma Process.*, 2007, **27**(5), p 609-623
15. C. Moreau, M. Lamontagne, and P. Cielo, Method and Apparatus for Monitoring the Temperature and Velocity of Plasma Sprayed Particles, USA Patent 5,180,921, 2003
16. S. Sampath and J. Matejicek, Method and Apparatus for Determining Process-induced Stresses and Elastic Modulus of Coatings by In Situ Measurement, USA Patent 6,478,875, 2002
17. J. Matejicek and S. Sampath, In Situ Measurement of Residual Stresses and Elastic Moduli in Thermal Sprayed Coatings—Part 1: Apparatus and Analysis, *Acta Mater.*, 2003, **51**(3), p 863-872
18. J. Matejicek, S. Sampath, D. Gilmore, and R. Neiser, In Situ Measurement of Residual Stresses and Elastic Moduli in Thermal Sprayed Coatings—Part 2: Processing Effects on Properties of Mo Coatings, *Acta Mater.*, 2003, **51**(3), p 873-885